doi:10.1093/brain/awab052

BRAIN
A JOURNAL OF NEUROLOGY

ATP1A2- and *ATP1A3*-associated early profound epileptic encephalopathy and polymicrogyria

Annalisa Vetro,[1] Hang N. Nielsen,[2] Rikke Holm,[2] Robert F. Hevner,[3] Elena Parrini,[1] Zoe Powis,[4] Rikke S. Møller,[5,6] Cristina Bellan,[7] Alessandro Simonati,[8] Gaétan Lesca,[9] Katherine L. Helbig,[10] Elizabeth E. Palmer,[11,12] Davide Mei,[1] Elisa Ballardini,[13] Arie Van Haeringen,[14] Steffen Syrbe,[15] Vincenzo Leuzzi,[16] Giovanni Cioni,[17] Cynthia J. Curry,[18] Gregory Costain,[19] Margherita Santucci,[20,21] Karen Chong,[22] Grazia M. S. Mancini,[23] Jill Clayton-Smith,[24] ATP1A2/ A3-collaborators,‡ Stefania Bigoni,[25] Ingrid E. Scheffer,[26] William B. Dobyns,[27,†] Bente Vilsen[2,†] and Renzo Guerrini[1,†]

†These authors contributed equally to this work.

‡Appendix 1.

Constitutional heterozygous mutations of *ATP1A2* and *ATP1A3*, encoding for two distinct isoforms of the Na^+/K^+-ATPase (NKA) alpha-subunit, have been associated with familial hemiplegic migraine (*ATP1A2*), alternating hemiplegia of childhood (*ATP1A2/A3*), rapid-onset dystonia-parkinsonism, cerebellar ataxia-areflexia-progressive optic atrophy, and relapsing encephalopathy with cerebellar ataxia (all *ATP1A3*). A few reports have described single individuals with heterozygous mutations of *ATP1A2/A3* associated with severe childhood epilepsies. Early lethal hydrops fetalis, arthrogryposis, microcephaly, and polymicrogyria have been associated with homozygous truncating mutations in *ATP1A2*. We investigated the genetic causes of developmental and epileptic encephalopathies variably associated with malformations of cortical development in a large cohort and identified 22 patients with *de novo* or inherited heterozygous *ATP1A2/A3* mutations. We characterized clinical, neuroimaging and neuropathological findings, performed *in silico* and *in vitro* assays of the mutations' effects on the NKA-pump function, and studied genotype-phenotype correlations. Twenty-two patients harboured 19 distinct heterozygous mutations of *ATP1A2* (six patients, five mutations) and *ATP1A3* (16 patients, 14 mutations, including a mosaic individual). Polymicrogyria occurred in 10 (45%) patients, showing a mainly bilateral perisylvian pattern. Most patients manifested early, often neonatal, onset seizures with a multifocal or migrating pattern. A distinctive, 'profound' phenotype, featuring polymicrogyria or progressive brain atrophy and epilepsy, resulted in early lethality in seven patients (32%). *In silico* evaluation predicted all mutations to be detrimental. We tested 14 mutations in transfected COS-1 cells and demonstrated impaired NKA-pump activity, consistent with severe loss of function. Genotype-phenotype analysis suggested a link between the most severe phenotypes and lack of COS-1 cell survival, and also revealed a wide continuum of severity distributed across mutations that variably impair NKA-pump activity. We performed neuropathological analysis of the whole brain in two individuals with polymicrogyria respectively related to a heterozygous *ATP1A3* mutation and a homozygous *ATP1A2* mutation and found close similarities with findings suggesting a mainly neural pathogenesis, compounded by vascular and leptomeningeal abnormalities. Combining our report with other studies, we estimate that ~5% of mutations in *ATP1A2* and 12% in *ATP1A3* can be associated with the severe and novel phenotypes that we describe here. Notably, a few of these mutations were associated with more than one phenotype. These findings assign novel, 'profound' and early lethal phenotypes of developmental and epileptic encephalopathies and polymicrogyria to the phenotypic spectrum associated with heterozygous *ATP1A2/A3* mutations and indicate that severely impaired NKA pump function can disrupt brain morphogenesis.

Received August 14, 2020. Revised December 08, 2020. Accepted December 09, 2020.
© The Author(s) (2021). Published by Oxford University Press on behalf of the Guarantors of Brain. All rights reserved.
For permissions, please email: journals.permissions@oup.com

Downloaded from https://academic.oup.com/brain/advance-article/doi/10.1093/brain/awab052/6242725 by Universita degli Studi di Ferrara - Biblioteca S. Maria delle Grazie user on 27 April 2021

1 Pediatric Neurology, Neurogenetics and Neurobiology Unit and Laboratories, Meyer Children's Hospital, University of Florence, Florence, Italy
2 Department of Biomedicine, Aarhus University, DK-8000, Aarhus C, Denmark
3 Department of Pathology, University of California San Diego, San Diego, CA, USA
4 Ambry Genetics, Aliso Viejo, CA, USA
5 Department of Epilepsy Genetics and Personalized Medicine Danish Epilepsy Centre, Filadelfia, Denmark
6 Department of Regional Health Services, University of Southern Denmark, Odense, Denmark
7 Department of Neonatal Intensive Care Unit, Bolognini Hospital, ASST-Bergamo Est, Seriate, Italy
8 Neurology (Child Neurology and Neuropathology), Department of Neuroscience, Biomedicine and Movement, University of Verona, Verona, Italy
9 Department of Medical Genetics, Member of the ERN EpiCARE, University Hospital of Lyon, Lyon, France
10 Division of Neurology, Children's Hospital of Philadelphia, Philadelphia, PA, USA
11 Centre for Clinical Genetics, Sydney Children's Hospital, Randwick, NSW, Australia
12 School of Women's and Children's Health, University of New South Wales, Randwick, NSW, Australia
13 Neonatal Intensive Care Unit, Pediatric Section, Department of Medical Sciences, Ferrara University, Ferrara, Italy
14 Department of Clinical Genetics, Leiden University Medical Center, Leiden, The Netherlands
15 Division of Pediatric Epileptology, Centre for Paediatrics and Adolescent Medicine, University Hospital Heidelberg, Heidelberg, Germany
16 Department of Human Neuroscience, Unit of Child Neurology and Psychiatry, Sapienza University, Rome, Italy
17 Department of Developmental Neuroscience, IRCCS Fondazione Stella Maris, Pisa, Italy
18 Genetic Medicine, Department of Pediatrics, University of California, San Francisco/Fresno, CA, USA
19 Division of Clinical and Metabolic Genetics, Department of Pediatrics, The Hospital for Sick Children, Toronto, Ontario, Canada
20 Child Neuropsychiatry Unit, IRCCS, Institute of Neurological Sciences, Bellaria Hospital, Bologna, Italy
21 DIBINEM, University of Bologna, Bologna, Italy
22 The Prenatal Diagnosis and Medical Genetics Program, Department of Obstetrics and Gynecology, Mount Sinai Hospital, University of Toronto, Toronto, ON, Canada
23 Department of Clinical Genetics, Erasmus MC University Medical Center, Rotterdam, The Netherlands
24 Manchester Centre for Genomic Medicine, University of Manchester, St Mary's Hospital, Manchester, UK
25 Medical Genetics Unit, Department of Mother and Child, Ferrara University Hospital, Ferrara, Italy
26 University of Melbourne, Austin Health and Royal Children's Hospital, Florey and Murdoch Institutes, Melbourne, Australia
27 Department of Pediatrics (Genetics), University of Minnesota, Minneapolis, MN, USA

Correspondence to: Prof. Renzo Guerrini
Neuroscience Department, Children's Hospital Anna Meyer-University of Florence
Viale Pieraccini 24, 50139 Florence
Italy. E-mail: r.guerrini@meyer.it

Correspondence (neuropathology) may also be addressed to: Robert F. Hevner
Department of Pathology, University of California San Diego
San Diego, CA
USA. E-mail: rhevner@ucsd.edu

Keywords: ATP1A2; ATP1A3; developmental and epileptic encephalopathy; polymicrogyria; Na + /K + -ATPase pump

Abbreviations: AHC = alternating hemiplegia of childhood; DEE = developmental and epileptic encephalopathy; FHM = familial hemiplegic migraine; NKA = Na^+/K^+-ATPase

Introduction

The Na^+/K^+-ATPase (NKA) ion pump is a ubiquitous transmembrane enzyme responsible for active exchange of Na^+ and K^+ ions across the plasma membranes of higher eukaryotic cells.[1] In neural tissue, this process is pivotal for maintaining the resting membrane potential, excitability, and secondary active transport that involves Na^+/H^+ and Na^+/Ca^{2+} exchange, K^+/Cl^- cotransport, and Na^+-dependent neurotransmitter uptake.[2] The NKA pump transports three Na^+ ions out of the cell and two K^+ ions into the cell for each ATP hydrolysed, undergoing large conformational changes between two principal conformations (E1 and E2) and their phosphorylated intermediates (E_1P and E_2P).[1-3] It is composed of a large catalytic α-subunit and smaller β- and γ-subunits. The α-subunit contains binding sites for three Na^+ ions in the E1 conformation or two K^+ ions in the E2 conformation, as well as a catalytic site that binds ATP and phosphate. The β-subunit is required for protein folding and targeting the α-subunit to the plasma membrane, while both β- and γ-subunits act as fine modulators of ion affinity in different tissues.[2]

The four known human isoforms of the α-subunit (α1–4) encoded by four paralogous genes (*ATP1A1–4*) share

Downloaded from https://academic.oup.com/brain/advance-article/doi/10.1093/brain/awab052/6242725 by Universita degli Studi di Ferrara - Biblioteca S. Maria delle Grazie user on 27 April 2021

84–91% of the amino acid sequence and have developmental and tissue expression specificity. The isoforms differ in affinity for Na^+, K^+ and ATP, and have different enzyme kinetics.[4] The α2- and α3-isoforms, encoded by *ATP1A2* and *ATP1A3*, are predominantly expressed in CNS. The expression of both isoforms is primarily neuronal during embryonic development. In the adult brain, α3 maintains its neuronal expression while α2 is primarily expressed in glial cells.[5,6] Multiple isoforms of β and γ regulatory subunits also exist, with different tissue distribution and functional effects.

Constitutional heterozygous mutations of *ATP1A2/A3* have been associated with several autosomal dominant neurological disorders with limited overlap. These include familial hemiplegic migraine (FHM; *ATP1A2*, MIM#602481); rapid-onset dystonia-parkinsonism (RDP; *ATP1A3*, MIM#128235); alternating hemiplegia of childhood (AHC; *ATP1A3*, MIM #614820 and a single family with an *ATP1A2* mutation)[7,8] cerebellar ataxia-areflexia-progressive optic atrophy (CAPOS; *ATP1A3*, MIM#601338); and relapsing encephalopathy with cerebellar ataxia (RECA; *ATP1A3*).[9] Epilepsy and intellectual disability may co-occur with AHC and FHM, and severe epilepsies have been described in rare patients with *ATP1A2* or *ATP1A3* mutations.[10,11] Early lethal hydrops fetalis, intrauterine growth restriction, arthrogryposis, microcephaly, polymicrogyria, and lack of respiratory drive have been associated with homozygous truncating mutations in *ATP1A2*.[12,13]

In this study, we describe a spectrum of severe neurodevelopmental phenotypes associated with heterozygous mutations of either *ATP1A2* or *ATP1A3* that may include early lethality, most often occurring during status epilepticus, microcephaly and the cortical malformation polymicrogyria as well as progressive brain atrophy. Combined with prior reports of FHM, RDP, AHC, CAPOS and RECA, our data define a wide spectrum of disorders that we designate 'ATP1A2/A3-opathies'. We explore the detrimental effects of causative mutations on NKA pump function using several different experimental paradigms and show that the most severe phenotypes are caused by mutations that are lethal in mammalian cell culture (COS-1 cells). We also demonstrate that neuropathological features of polymicrogyria associated with heterozygous *ATP1A3* and biallelic *ATP1A2* mutations are similar and support a mainly neural pathogenesis, compounded by vascular abnormalities.

Materials and methods

Patients

Our initial discovery cohort consisted of 2800 individuals referred to the Neuroscience and Neurogenetics Department of the Meyer Children's Hospital to investigate the genetic causes of developmental and epileptic encephalopathies (DEEs, defined according to Scheffer et al.).[14] Within this cohort, we identified *de novo* and inherited heterozygous mutations of *ATP1A2* and *ATP1A3* in nine patients (Patients 3, 6, 9, 11, 12, 14–16, and 20). Alerted by this association, we identified another 13 patients with similar features through international collaborations and by interrogating the DECIPHER database (http://decipher.sanger.ac.uk) (Patients 1, 2, 4, 5, 7, 8, 10, 13, 17–19, 21 and 22). We obtained written informed consent from all participants or their legal guardians according to local requirements. The study was approved by the Pediatric Ethics Committee of the Tuscany Region (grant 602531). We reviewed medical records, ECG, EEGs, and brain MRI scans. Seizure types were classified following ILAE criteria[14] whenever applicable and used more descriptive terms when seizure phenomenology could not be easily classified using classification terminology. We submitted all novel mutations to DECIPHER. One child with a biallelic mutation of *ATP1A2* (Patient 23) was described clinically in a prior report.[13] Here we report brain autopsy findings and compare them to another child in this cohort.

Detailed materials and methods for MRI investigations, brain neuropathology in Patients 11 and 23, genetic analysis, homology modelling and structural analysis, and functional characterization of *ATP1A2* and *ATP1A3* heterozygous mutations are reported in the Supplementary material.

Data availability

The authors confirm that the data supporting the findings of this study are available within the article and its Supplementary material. Any additional raw data are available on request from the corresponding author.

Results

Clinical description

Clinical and genetic data for 22 patients (11 males/11 females) with 19 heterozygous mutations in *ATP1A2* ($n = 6$, Patients 1–6) or *ATP1A3* ($n = 16$, Patients 7–22) are summarized in Table 1 and Supplementary Table 1; data for Patient 23 who carries a biallelic *ATP1A2* mutation and was not considered in the clinical study, is also included.

Epilepsy was reported in 21/22 individuals, with seizure onset during the neonatal period in 11 individuals and during infancy or childhood in the remaining 10. Refractory status epilepticus had occurred in 10 patients, in five of whom as the presenting type of seizure in the neonatal period (Patients 3, 4, 7, 11 and 13). Most had multiple seizure types, with multifocal ($n = 9$) and focal seizures ($n = 7$) being most frequent. The multifocal seizure pattern observed in these patients corresponded to the epilepsy of infancy with migrating focal seizures (EIMFS) syndrome.[15] Recurrent, prolonged, seizure-related apnoeic episodes, accompanied by intense cyanosis, were a prominent feature in eight patients (Patients 3, 7, 11, 12, 16, 17, 20 and 21). In two additional neonates, apnoeic episodes were attributed to central apnoeas (Patients 14 and 18). A burst suppression EEG pattern was documented in two children (Patients 3 and 11).

Downloaded from https://academic.oup.com/brain/advance-article/doi/10.1093/brain/awab052/6242725 by Universita degli Studi di Ferrara - Biblioteca S. Maria delle Grazie user on 27 April 2021

Table 1 Schematic representation of the main clinical features in our cohort with structural location and functional effect of the corresponding mutations in *ATP1A2* (A2) and *ATP1A3* (A3)

Patient/ mutation		Phenotype					Location/function								
Pt#	Variant	Died 0–3 y	DD/ID	MIC (subtype)	PMG	AH	Structural location	Cell survival[a]	Phos.	Max TO rate	NKA activity/mg membrane protein	Na^+ affinity	Na^+/K^+ selectivity	K^+ affinity	Conformational change	
															E1–E2	E1P–E2P
Group 1 Variant does not support cell survival in culture (this study; *n* = 9 mutations in 11 patients)																
2	A2-C341F	No	SEV	No	No	No	M4	No	10–15%	–	–	–	–	–	–	–
3	A2-G366A	Yes	SEV	No	No	No	P	No	61%	–	–	↓ 3–5-fold	–	↓ >15-fold	–	Shift E1P→→E2P
4	A2-G366A	Yes	SEV	MIC (P)*	No	No	P	No	61%	–	–	↓ 3–5-fold	–	↓ >15-fold	–	Shift E1P→→E2P
7	A3-L292R	Yes	SEV	MIC (P)**	Yes	No	M3	No	61%	–	–	↓ 3–5-fold	–	↓ >15-fold	–	–
8	A3-G316V	No	SEV	No	No	No	M4	No	70%	–	–	↑ 4-fold	–	↓ >15-fold	–	–
9	A3-S361P	No	MOD	MIC (P)**	No	No	P	No	10–15%	–	–	–	–	–	–	–
20	A3-S361P	No	NA	MIC (C)**	Yes	Yes	P	No	10–15%	–	–	–	–	–	–	–
11	A3-K764del	Yes	SEV	MIC (C)**	Yes	No	M5	No	10–15%	–	–	–	–	–	–	–
12	A3-P775R	No	SEV	No	No	No	M5	No	∼0%	–	–	–	–	–	–	–
16	A3-L888P	No	SEV	No	Yes	Yes	L7–8	No	∼0%	–	–	–	–	–	–	–
19	A3-D992dup	Yes	NA	MIC (P)	Yes	No	M10	No	∼0%	–	–	–	–	–	–	–
		5/11	8/9 SEV	6/11	5/11	2/11										
Group 2 - Variant does support cell survival in culture (this study; *n* = 5 mutations in six patients)																
1	A2-I293M	No	MOD	No	No	No	M3	Yes	>50%	27%	∼17%	↓ 3–5-fold	↓	–	Shift E2→→E1	Shift E2P→→E1P
5	A2-R593Q	No	No	No	No	No	P	Yes	>50%	42%	∼36%	∼WT	↓	–	Shift E2→E1	Shift E2P→E1P
6	A2-R908Q	No	MOD	MIC (P)**	Yes	No	L7–8	Yes	∼26%	84%	∼22%	∼WT	–	–	Shift E1→E2	–
14	A3-D887Y	No	SEV	No	Yes	No	L7–8	Yes	∼35%	95%	∼33%	∼WT	↓	–	Shift E2→E1	–
15	A3-D887Y	No	MILD	No	Yes	No	L7–8	Yes	∼35%	95%	∼33%	∼WT	↓	–	Shift E2→E1	–
18	A3-P972del	Yes	SEV	No	No	No	L9–10	Yes	∼35%	85%	∼30%	↓ Slightly	↑	–	Shift E1→E2	Shift E2P→E1P
		1/6	2/6 SEV	1/6	3/6	0/6										

We separated the 17 patients (14 mutations) for whom experimental data were available from this study into two groups based on COS-1 cell survival under ouabain selection pressure. The mutations are distributed across the following locations: phosphorylation domain (P), transmembrane helices (M3–10) and their intervening loops (L). Nine different aspect of the NKA pump function investigated by at least one of the different experimental approaches are showed. AH = alternating hemiplegia; DD/ID = developmental delay/intellectual disability; MIC = microcephaly (–2 SD*; >–3 SD**; no asterisk means there is microcephaly but standard deviations are unknown; C = congenital; P = postnatal); MOD = moderate; NA = not applicable/not available; Phos. = phosphorylation; PMG = polymicrogyria; SEV = severe; TO = turnover; WT = wild-type.

[a]Cell survival under ouabain selection.

Downloaded from https://academic.oup.com/brain/advance-article/doi/10.1093/brain/awab052/6242725 by Universita degli Studi di Ferrara - Biblioteca S. Maria della Grazie user on 27 April 2021

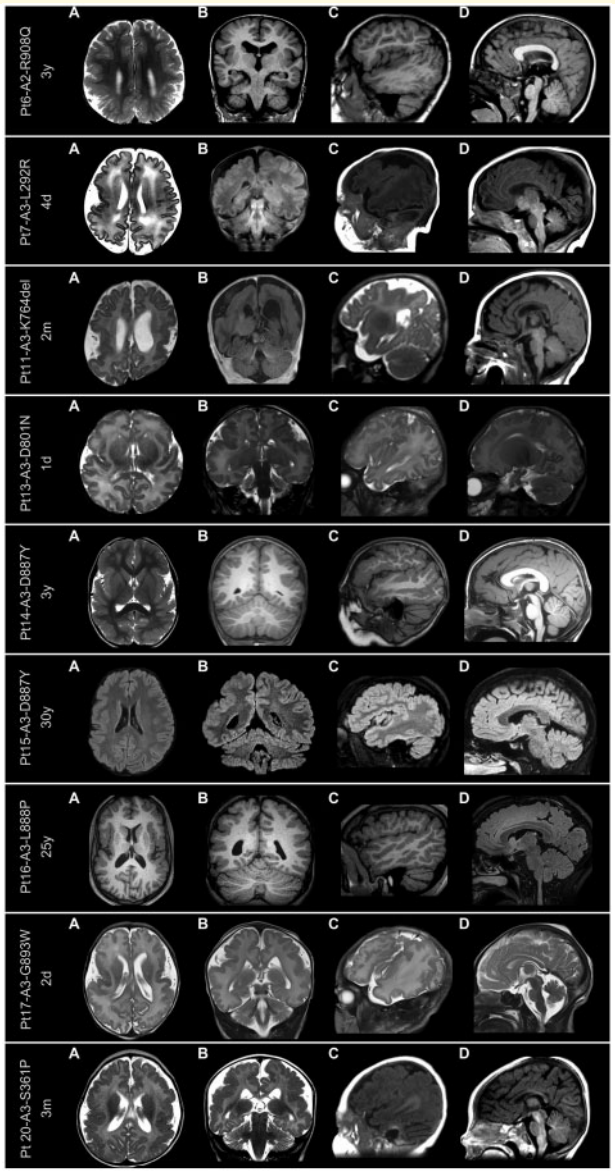

Figure 1 Brain MRI in nine patients with polymicrogyria. From *top* to *bottom*: Representative brain MRI findings in Patients 6, 7, 11, 13–17 and 20 with an indication of the mutations and age at which imaging was performed. For each patient four cuts are presented, which include axial (column **A**), coronal (column **B**), sagittal through the Sylvian fissure (column **C**), and sagittal through the midline (column **D**) images. Sequences are at 1.5 to 3 T and include T_1-weighted, T_2-weighted and fluid-attenuated inversion recovery (FLAIR) images. All patients have polymicrogyria with abnormal cortical infoldings and packed microgyri, combined with abnormal sulcation. A recurrent feature, present in all patients, is an abnormal Sylvian fissure with thickened cortex, pronounced infolding and vertically oriented axis. These abnormalities are better visible in column **A** (enlarged Sylvian space), column **B** (infolding) and column **C** (cortical thickening and verticalized Sylvian fissure). There are some differences in individual patients. In Patient 6, polymicrogyria is diffuse and more prominent posteriorly. In Patient 7, the cortical abnormality is asymmetrical, due to a smaller right hemisphere. In Patient 11 too, there is asymmetry with the right hemisphere being more severely affected and smaller. In Patients 13, 14, 16 and 17, polymicrogyria is almost exclusively bilateral perisylvian, sparing the remaining cortex. In Patient 15 too, who is the mother of Patient 14, the cortical abnormality is perisylvian but unilateral only involving the right hemisphere. In Patient 17, there is diffuse polymicrogyria with more severe perisylvian involvement. In line **D**, midline cuts show thickening of the corpus callosum in Patients 6, 14 and 15. There is some degree of vermian hypoplasia in Patients 7 and 17.

Multiple antiseizure medications were used both in the acute treatment of status epilepticus/prolonged seizures and as chronic treatments, with no evidence of any drug being more effective than any other or causing seizure worsening.

Survival was often short; eight children died due to complications of status epilepticus (Patients 3, 4, 7, 10, 11, 17, 19), or intercurrent respiratory infections (Patient 18); seven of these children died between 10 days and 30 months of life (Patients 3, 4, 7, 11 and 17–19) and one at 14 years (Patient 10). Overall, four children died within the first 2 months of life (Patients 4, 7, 17 and 19), too early to detect progressive worsening, which was instead apparent in the remaining four who died at a later age.

ECG data, available for 19 children (*ATP1A2*: Patients 2–4 and 6; *ATP1A3*: Patients 7–14 and 16–22) were unremarkable in all, except Patient 13 in whom a short QT interval with unusual ST segment was reported, which had remained asymptomatic at age 3 years (Supplementary Table 1).

Severe congenital or postnatal (usually by age 2 years) microcephaly was observed in 10/22 patients. Global developmental delay and intellectual disability was documented in 18/22 patients, including all who survived long enough to be assessed. The disability was rated as severe to profound in 14, moderate in three, and mild in 1/18 patients. Severe axial hypotonia was reported in 14 individuals including three with dyskinetic quadriparesis (Patients 2, 10 and 18). Attacks of alternating hemiplegia were observed in only two children (Patients 16 and 20), both having polymicrogyria. Additional clinical findings in this cohort included Pierre-Robin sequence (micrognathia with cleft palate, Patient 11), optic nerve atrophy (Patient 10), and hypogenetic lung syndrome (Patient 14).

Brain imaging

All 22 patients with *ATP1A2/A3* heterozygous mutations had at least one brain MRI scan and six were scanned more than once at greater than 1-year intervals. The main finding, observed in 10 patients (45%), was polymicrogyria (nine *ATP1A3* mutations: Patients 7, 11, 13–16, 17, 19 and 20; one *ATP1A2* mutation: Patient 6), which was perisylvian predominant, bilateral in nine patients and unilateral in one (Patient 15), inconstantly involving other areas (Fig. 1). Perisylvian involvement was accompanied in all by severe disruption of the sulcal pattern, with a vertically-oriented and extended Sylvian fissure. Associated findings included microcephaly in 7/10 and thick corpus callosum in 4/10 patients (Supplementary Table 1 and Fig. 1). Two subjects

Downloaded from https://academic.oup.com/brain/advance-article/doi/10.1093/brain/awab052/6242725 by Universita degli Studi di Ferrara - Biblioteca S. Maria delle Grazie user on 27 April 2021

with polymicrogyria had repeated brain MRI studies that showed no signs of progressive changes.

Severe and progressive brain atrophy was instead documented in two patients, without polymicrogyria (Patients 2 and 8; Supplementary Fig. 1). In the 10 remaining patients, brain MRI was normal or showed mild atrophic changes, and remained so in the two who were scanned twice (Patients 9 and 10).

Neuropathological brain examination

In Patient 11, with a heterozygous *ATP1A3* mutation (A3-K764del), and in Patient 23, with a homozygous *ATP1A2* frameshift mutation (A2-R279G*4), we performed post-mortem neuropathological examination and compared findings (Figs 2 and 3).

The brain of Patient 11 appeared small for the age of four postnatal months (brain weight not available). The surface gyri were abnormal, mostly small and irregular, but with apparent pachygyria of pericentral cortex bilaterally, and bilateral widening of the central sulcus (Fig. 2A–C). In slices, the corpus callosum was present but small at the genu and was truncated with lack of midline crossing at the level of the posterior body and splenium, thus forming Probst bundles (Fig. 2G). The regions of surface pachygyria showed abnormally thick cortical grey matter (Fig. 2D and E). Hemispheric white matter was also reduced. The basal ganglia and thalami appeared relatively spared, with almost normal size. The cerebellar folia showed no obvious defects. The cerebellar dentate nuclei and the inferior olives had simplified morphology, and no arcuate nuclei were detected. Histology revealed that the macroscopically pachygyric cortex was thick, disorganized, and partially covered by rinds of leptomeningeal glioneuronal heterotopia (Fig. 2F and G). Histology also demonstrated that the macroscopic appearance of pachygyria actually corresponded to disorganized layers with some features of classic four-layered polymicrogyria (Fig. 2F and G, arrowheads); the pachygyric appearance was conferred in part by the rind of leptomeningeal heterotopia. Some areas exhibited more definitive features of polymicrogyria (Fig. 2F and G, arrows), while other areas showed essentially normal cortical lamination. Overall, these findings indicated a variable malformation of cortical development affecting central regions more severely that was also associated with malformations of brainstem and cerebellar nuclei.

The brain of Patient 23 was very small for the age of 33 gestational weeks (91.5 g; expected 220 g). Surface gyri were difficult to assess due to adherent meninges with subarachnoid haemorrhage (agonal) and congested blood vessels (Fig. 3A and B). Midline section revealed that the corpus callosum was small but present, including the splenium (arrow Fig. 3B). The cerebellum was moderately hypoplastic, with reduced foliation (Fig. 3C). Coronal slices through the hemispheres revealed severe hypoplasia of gray and white structures, as well as moderate enlargement of the posterior lateral ventricles (i.e. colpocephaly: Fig. 3D–F). The cortical gyri were diffusely small with extensive folding, suggestive of polymicrogyria, except for the hippocampus, which appeared relatively normal bilaterally (Fig. 3E, arrows). Histology confirmed diffuse polymicrogyria throughout the cortex except in the hippocampus, which displayed relatively normal lamination (Fig. 3G and H). Leptomeningeal glioneuronal heterotopia were widespread over the external surface of the hemispheres (Fig. 3I). Histology also revealed abundant focal calcifications (or mineralization) involving cerebral grey and white matter, leptomeninges and blood vessels (Fig. 3G–L, arrows). Some blood vessels had abnormally thick walls (intimal hyperplasia) as well as mineralizations (Fig. 3L). Also, the cerebellar deep nuclei were dysplastic, and the pyramidal tracts were severely hypoplastic (not shown).

Genetic findings

We identified 19 heterozygous mutations of *ATP1A2* ($n = 5$) or *ATP1A3* ($n = 14$; Supplementary Table 1) including 15 missense substitutions, three in-frame deletions, and one insertion. All 19 mutations affected highly conserved residues among both orthologs and paralogues of *ATP1A2* and *ATP1A3* (Supplementary Table 1 and Supplementary Fig. 2) and were interpreted as pathogenic based on both *in silico* analysis using sequence data and the functional studies described below. Two mutations (A2-G366A and A3-S361P) were recurrent, occurring in two individuals each. The mutations occurred *de novo* in 20/22 patients and were inherited in two individuals from one family (Patients 14 and 15: A3-D887Y). The latter was inherited across three generations from a reportedly healthy male to his daughter (Patient 15) and grandson (Patient 14). None of the mutations were present in either gnomAD or our internal dataset.

Analysis of the variant allele frequency (VAF) showed that 21/22 mutations were constitutional and one mosaic with VAF 26.2%. Eleven heterozygous mutations were novel (*ATP1A2* $n = 2$; *ATP1A3* $n = 9$; Supplementary Table 1). Of the eight mutations previously reported, three were associated with FHM (Patient 6: A2-R908Q) or AHC (Patient 10: A3-D609Y; Patient 13: A3-D801N).[16-19] The mosaic mutations found in our series (Patient 21: A3-F857del) was reported as a constitutional mutation with no clinical details in one individual.[20] Four additional mutations found in Patients 1, 3, 16 and 22 reported here had been mentioned in previous series within which these patients had been included.[15,21-23] No additional potentially pathogenic mutations were identified in the 20 patients with available whole-exome/whole genome sequencing (WES/WGS) data and in the two examined by targeted gene panel (Patients 2 and 5).

Homology modelling and structural analysis

Of the 19 mutations in our cohort, eight *ATP1A3* mutations, but only two *ATP1A2* mutations, affected the

Downloaded from https://academic.oup.com/brain/advance-article/doi/10.1093/brain/awab052/6242725 by Universita degli Studi di Ferrara - Biblioteca S. Maria delle Grazie user on 27 April 2021

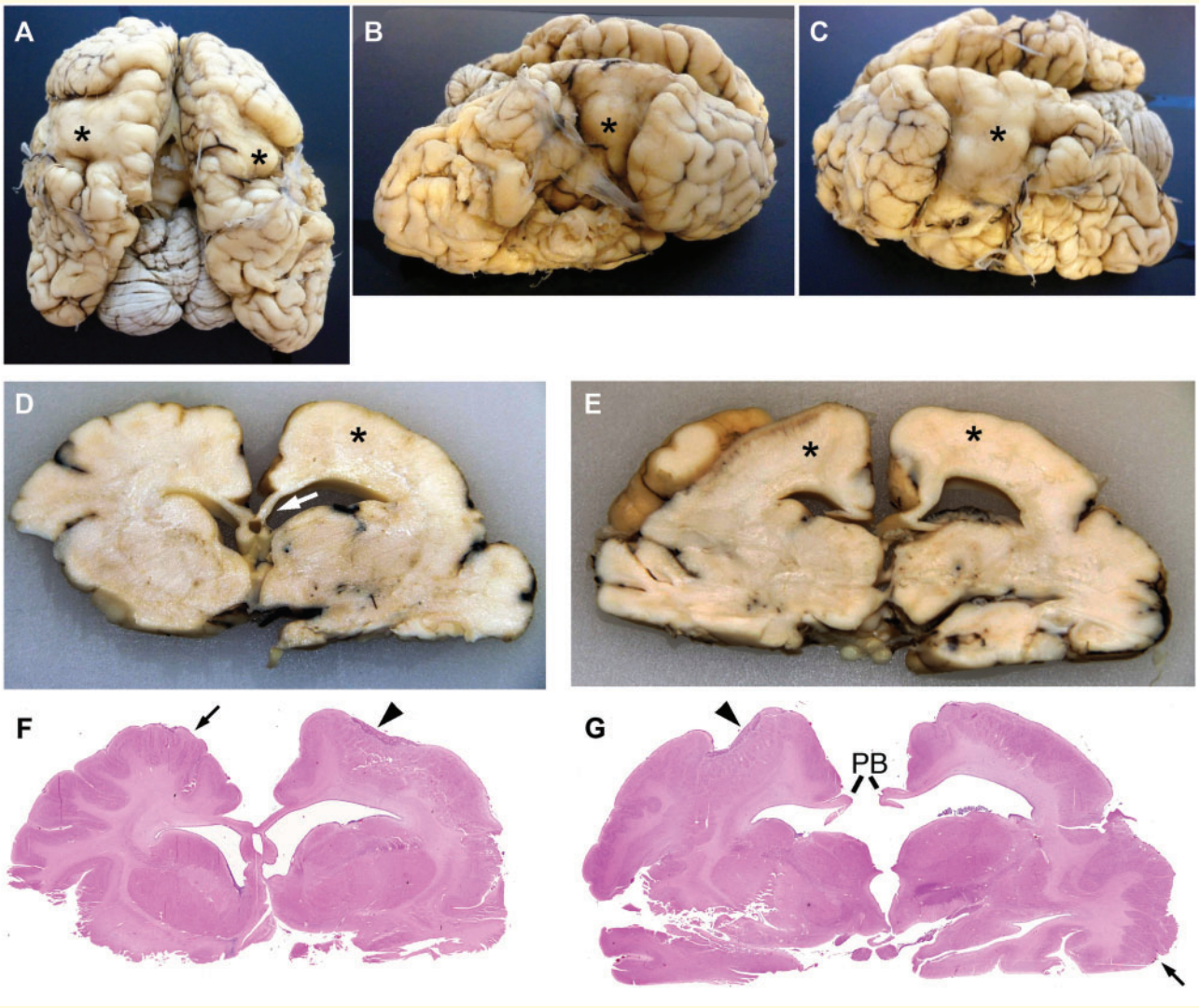

Figure 2 Neuropathology of Patient 11, age 4 months (A3-K764del). (**A**–**C**) Macroscopic views of the brain from (**A**) posterior, (**B**) right, and (**C**) left sides demonstrated overall small cerebral hemispheres, with externally apparent pachygyria (asterisks) involving pericentral cortex bilaterally. (**D** and **E**) Coronal slices through (**D**) anterior and (**E**) middle regions of the hemispheres showed thick cortex corresponding to externally apparent pachygyria (asterisks), and thin but intact genu of the corpus callosum (**D**, white arrow). (**F** and **G**) Histology of the brain slices demonstrated leptomeningeal glioneuronal heterotopia (black arrowheads) covering cortex that appeared externally pachygyric, but histologically showed features of four-layered polymicrogyria, also seen in other cortical areas (black arrows). Callosal fibres did not cross the midline posteriorly, but instead formed Probst bundles (PB).

transmembrane helices M3 (A3-L292R, A2-I293M), M4 (A3-G316V, A2-C341F), M5 (A3-K764del, A3-P775R), M6 (A3-D801N), M7 (A3-F857del), M8 (A3-L924P), and M10 (A3-D992dup) (Fig. 4 and Supplementary Fig. 3). The predicted structural impacts of all mutations in our cohort are detailed in Supplementary Table 2 and illustrated in Supplementary Figs 4–10. A3-D801N has previously been shown to impair Na^+ and K^+ transport as D801 is known to directly bind Na^+ and K^+ at both sites I and II.[3,24,25] A3-L924P is predicted to break the M8 helix, thereby indirectly disturbing the interaction of the juxtaposed D923 with Na^+ at site III.[26] The mutations A3-L292R, A2-I293M, A3-G316V, A2-C341F, A3-K764del, A3-P775R, A3-L924P, and A3-D992dup found in transmembrane helices and A3-P972del in the L8-9 loop connecting the transmembrane helices M8 and M9 are predicted to affect the ion binding sites indirectly. Four mutations affected the P domain, which contains the phosphorylation site (A2-G366A, A2-R593Q, A3-S361P, and A3-D609Y). A3-D609Y replaces the aspartate of the conserved TGD motif critical for ATP binding.[3] The remaining four mutations (A2-R908Q, A3-D887Y, A3-L888P, A3-G893W) affected the L7-8 extracellular loop between transmembrane helices M7 and M8, which interacts with the extracellular domain of the β-subunit. Hence, these mutations are predicted to interfere with the α-β interaction crucial to expression in the plasma

Downloaded from https://academic.oup.com/brain/advance-article/doi/10.1093/brain/awab052/6242725 by Universita degli Studi di Ferrara - Biblioteca S. Maria delle Grazie user on 27 April 2021

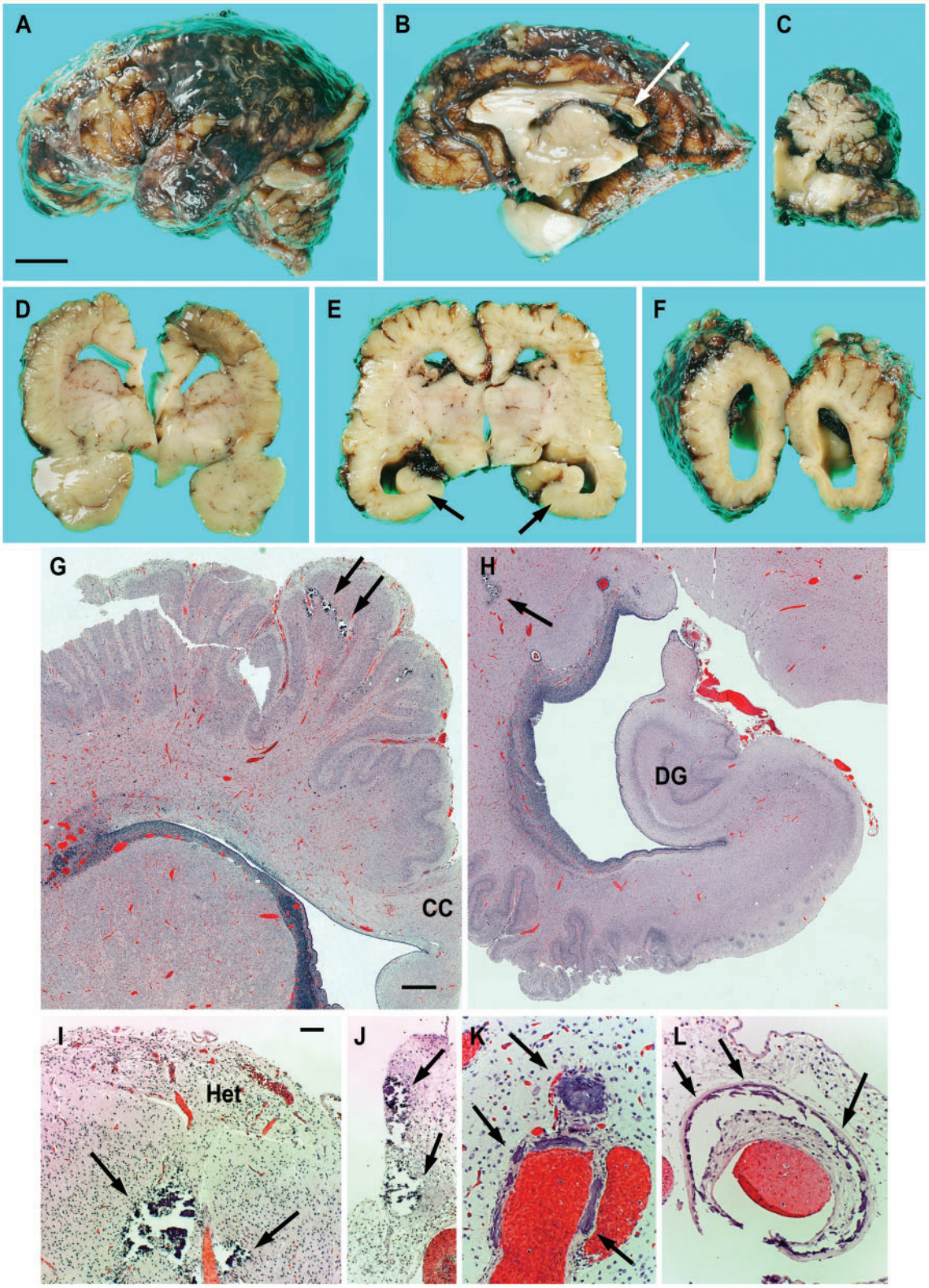

Figure 3 Neuropathology of Patient 23, age 1 day (A2-R279Gfs4*, homozygous). (**A**–**F**) Macroscopic brain abnormalities. (**A**) Left brain, lateral view. Blood vessels were congested; the leptomeninges contained subarachnoid haemorrhage (agonal) and were adherent to the brain surface. (**B**) Right hemisphere, medial view. The corpus callosum was thin (white arrow). (**C**) Brainstem and right cerebellum, medial view. The cerebellum was moderately hypoplastic. (**D** and **E**) Coronal slices of brain, (**D**) level of amygdala and (**E**) anterior hippocampus. The basal ganglia and thalamus were moderately hypoplastic; the cortex was diffusely polymicrogyric, except for the hippocampi (black arrows), which appeared relatively well-formed. (**F**) The occipital lobes (coronal slices) exhibited polymicrogyria and moderate colpocephaly. Histopathology (haematoxylin and eosin, G-N) (**G**) Frontal cortex, coronal section (midline right). The cortex was diffusely polymicrogyric, had an attached

(continued)

Downloaded from https://academic.oup.com/brain/advance-article/doi/10.1093/brain/awab052/6242725 by Universita degli Studi di Ferrara - Biblioteca S. Maria delle Grazie user on 27 April 2021

membrane. These four mutations were all associated with polymicrogyria. A3-G893W introduces a bulky tryptophan corresponding to the glycine of the SYGQ motif at the interface with the β-subunit. A3-F857del is likely to affect the interaction between M7 and the transmembrane helix of the β-subunit. No mutations involved the N-terminal third of the protein including M1-M2 and the A domain.

Functional characterization of *ATP1A2–A3* heterozygous mutations

The primary function of ATP driven NKA pumps is to rapidly exchange three intracellular Na^+ ions for two extracellular K^+ ions. In the presence of ATP and intracellular Na^+, the ATP-NKA pump in its E1 state forms a phosphorylated intermediate (E1P) that changes configuration from the E1P to E2P state, exposing Na^+ to the extracellular space. In the presence of extracellular K^+, three Na^+ are released and two K^+ bound (Fig. 5D). The phosphorylated intermediate (E2P) is hydrolysed to the E2 state which equilibrates to the E1 state in the presence of intracellular ATP, delivering two K^+ to the intracellular space.

Among the COS-1 cell lines transfected with the 14 mutations we tested, only three *ATP1A2* and two *ATP1A3* mutants retained the 5–10% wild-type NKA pump activity required for cell survival under ouabain selection.[3] The remaining two *ATP1A2* and seven *ATP1A3* mutants could not support cell growth in stable transfections, indicating that they lacked NKA pump activity or were not expressed in the plasma membrane (Table 1 and Supplementary Table 2). Hence, we analysed these mutants by transient transfection into COS-1 cells using siRNA to knock down the endogenous NKA pump, as described previously.[27]

Among the five stably expressed mutants retaining transport activity (cell survival), only A2-I293M and A2-R593Q showed phosphorylation levels >50% wild-type, whereas levels of A2-R908Q, A3-P972del, and A3-D887Y were 26-35% wild-type (Fig. 5A and Table 1). However, the turnover rate (rate of Pi liberation per active site in the presence of both Na^+ and K^+) was markedly reduced for A2-I293M (27% wild-type) and A2-R593Q (42% wild-type) (Fig. 5B and Table 1). Hence, the NKA pump activity calculated by multiplying the phosphorylation level by the turnover rate was markedly reduced for all five mutants (17–36% wild-type), thus accounting for the pathogenic effects of all five stably expressed mutations (Table 1).

Among the nine remaining mutants that could only be transiently expressed because of lack of NKA pump activity (Fig. 5C), the phosphorylation levels of A2-G366A (61%), A3-L292R (61%), and A3-G316V (70%) indicated that they were expressed in the plasma membrane and retained the ability to bind Na^+ and ATP, despite their inability to undergo the complete transport cycle.

To explore the Na^+- and K^+-binding properties of the mutants, we took advantage of the Na^+- and K^+-dependence of NKA phosphorylation and pump activity, which could be studied for the stably as well as the transiently expressed mutants showing robust phosphorylation. The effects of mutations on the E1-E2 and E1P-E2P conformational changes (*cf.* reaction cycle in Fig. 5D) are summarized in Fig. 6A, B, Supplementary Figs 11 and 12, with full text presentation in the Supplementary material. The very low or undetectable phosphorylation (expression) levels in the remaining six mutants (A2-C341F, A3-S361P, A3-K764del, A3-P775R, A3-L888P, and A3-P992dup), prevented further study of their phosphorylation properties (Fig. 5C).

In brief, the mutations in the transmembrane helices for which the ion binding properties could be examined (M3: A2-I293M and A3-L292R, M4: A3-G316V; Supplementary Figs 4 and 9), profoundly interfered with Na^+ and/or K^+ binding in various ways. Na^+ binding was also disturbed by one of the mutations in the P-domain (A2-G366A; Supplementary Fig. 6) and the mutation in the L9-10 loop (A3-P972del; Supplementary Fig. 10). In addition, A2-G366A disturbed K^+ binding, as the E2P phosphoenzyme intermediate of this mutant was completely insensitive to K^+. The M3 mutant (A2-I293M; Supplementary Fig. 4) had a strong conformational shift in favour of E1/E1P explaining the reduced turnover rate. A similar, but less strong conformational shift was seen for the P-domain mutation near the ATP binding site (A2-R593Q; Supplementary Fig. 7). The remaining mutations in transmembrane helices (A2-C341F, A3-K764del, A3-P775R, and A3-D992dup; Supplementary Figs 5, 9 and 10) resulted in low or undetectable phosphorylation levels, either due to inability to react with Na^+ and ATP to form a phosphoenzyme, or lack of expression of the mutant in the plasma membrane. The same was the case for the P-domain mutation (A3-S361P) located five residues from the phosphorylated aspartate (Supplementary Fig. 6). Mutations in the L7-8 loop, interacting with the β-subunit crucial to expression in the plasma membrane (Supplementary Fig. 8), also reduced the

Figure 3 continued

external rind of leptomeningeal glioneuronal heterotopia, and contained focal calcifications (arrows). The corpus callosum (CC) was small, but crossed the midline. (**H**) Medial temporal lobe, coronal section. The hippocampus was well-formed, including the dentate gyrus (DG), while neocortex was polymicrogyric. Focal calcifications (arrows) were noted in deep white matter. (**I**) Leptomeningeal glioneuronal heterotopia (Het) covered much of the cortical surface. Note focal parenchymal calcifications (arrows). (**J**) Leptomeninges with focal calcifications (arrows). (**K**) Cortical blood vessel with mineralized walls (arrows). (**L**) Meningeal blood vessel with medial calcifications (arrows), and intimal hyperplasia possibly due to thrombosis and recanalization. Scale bars = 1 cm in **A** for **A**–**F**); 1 mm in **G** for **G** and **H**); 100 μm in **I** for **I** and **J**; 50 μm in **I** for **K** and **L**).

Downloaded from https://academic.oup.com/brain/advance-article/doi/10.1093/brain/awab052/6242725 by Universita degli Studi di Ferrara - Biblioteca S. Maria delle Grazie user on 27 April 2021

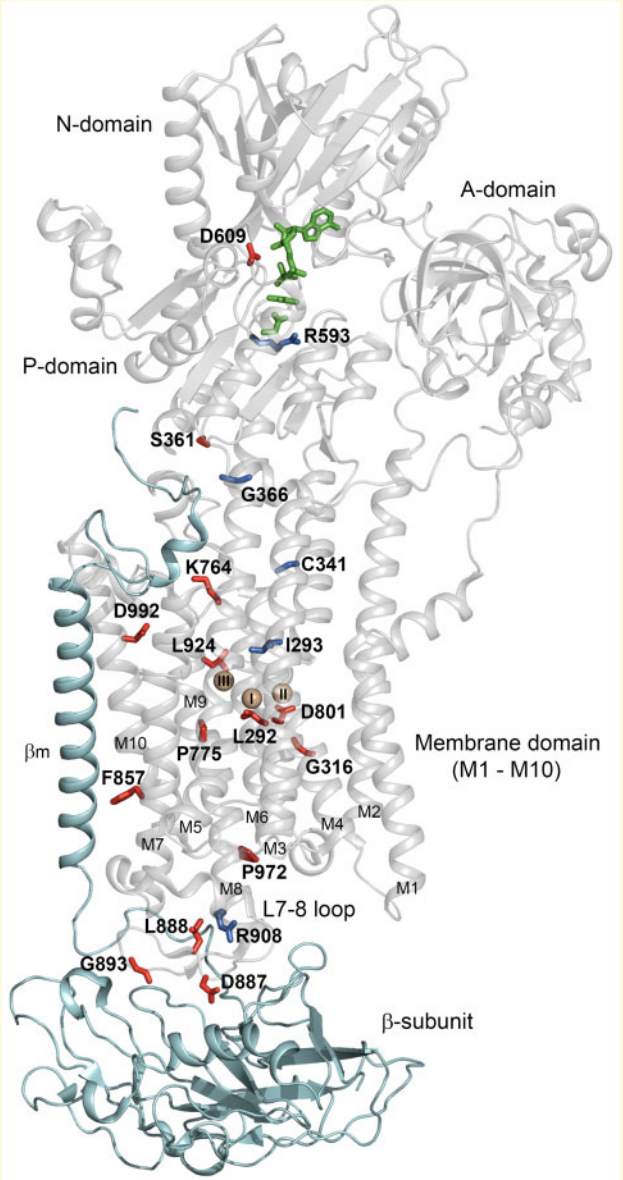

Figure 4 Overview of the structural location of ATP1A2 and ATP1A3 disease mutations in the cohort. The NKA α-subunit consists of three major cytoplasmic domains A ('actuator'), N ('nucleotide-binding'), and P ('phosphorylation') linked to a membrane domain composed of ten transmembrane helices (M1-M10) with their intervening loops on both membrane sides. The β-subunit (PDB ID 3WGV, chain B, teal colour) consists of a transmembrane helix βm and an extracellular domain that interacts with the α-subunit loop connecting M7 and M8 (L7-8 loop). Amino acid residues targeted by the mutations in the cohort are shown in blue (ATP1A2 mutations) and red (ATP1A3 mutations) in the structure of the ATP1A1 α-subunit in E1 form (PDB ID 3WGV, chain A, grey colour) with $3Na^+$ (golden spheres labelled I, II, and III according to common nomenclature) and ADP with phosphate analogue AlF_4 and the phosphorylated aspartate in green.

phosphorylation level, either partially (A3-D887Y and A2-R908Q) or completely (A3-L888P), most likely due to reduced expression.

In summary, in every patient whose mutations were tested at least one of the assays used showed severe impairment, as summarized in Table 1. The 11 mutations not supporting cell growth in culture were associated with the most severe clinical phenotype, while the five mutations supporting cell growth were associated with more variable clinical phenotypes.

Discussion

Since the first reports of *ATP1A2* and *ATP1A3* mutations in 2003–04[28,29] more than 200 mutations ($n = 92$ *ATP1A2*, $n = 136$ *ATP1A3*) have been identified [Human Gene Mutation Database (HGMD) Professional 2018.3, https://portal.biobase-international.com, last accessed June 2020]. Autosomal dominant disorders associated with *ATP1A3* mutations have been conceptualized as a phenotypic continuum that includes RDP, AHC, CAPOS, RECA, and DEE.[9,11,30] *ATP1A2* mutations have been associated with FHM and, in a single family, AHC,[7,8] defining a much narrower and less severe phenotype than *ATP1A3* (Fig. 7).

Here we describe 22 individuals with heterozygous *ATP1A2* or *ATP1A3* mutations associated with developmental encephalopathies manifesting most often as early-onset DEE, and associated with frequent early lethality (in 32%) and polymicrogyria (in 45%). Clinical and functional findings assign these novel, 'profound' phenotypes to the existing spectrum of disorders associated with heterozygous *ATP1A2/A3* mutations and demonstrate that severely impaired Na^+/K^+-pump function can disrupt brain morphogenesis.

Combining our report of 19 mutations (11 novel) with all prior reports, we estimate that ~5% of mutations in *ATP1A2* and 12% in *ATP1A3* are associated with the severe and novel phenotypes that we describe in this series. Notably, a few of these mutations were associated with more than one phenotype (Fig. 7).

Epilepsy

Epilepsy occurs in about 50% of patients with AHC and 15–30% of those with FHM.[16,18,31,32] In our cohort, which was assembled based on clinical features of developmental encephalopathy, epilepsy occurred in 21 of 22 patients (95%), with neonatal or early infantile onset in most and episodes of status epilepticus in 10 (45%). Status epilepticus has been reported to occur in up to 40% of patients with *ATP1A3*-AHC[21] but is a less frequent feature in *ATP1A2*-FHM.[31,32] The occurrence of multiple seizure types, especially multifocal seizures manifested as EIMFS, in most patients indicates widespread epileptogenesis and brain dysfunction. Patients 3 and 4 exhibited a remarkably severe phenotype among those with *ATP1A2* mutations reported so far, manifesting neonatal onset super-refractory status epilepticus featuring prolonged apnoeic episodes. Both patients died within the first year of life without achieving developmental or

Downloaded from https://academic.oup.com/brain/advance-article/doi/10.1093/brain/awab052/6242725 by Universita degli Studi di Ferrara - Biblioteca S. Maria delle Grazie user on 27 April 2021

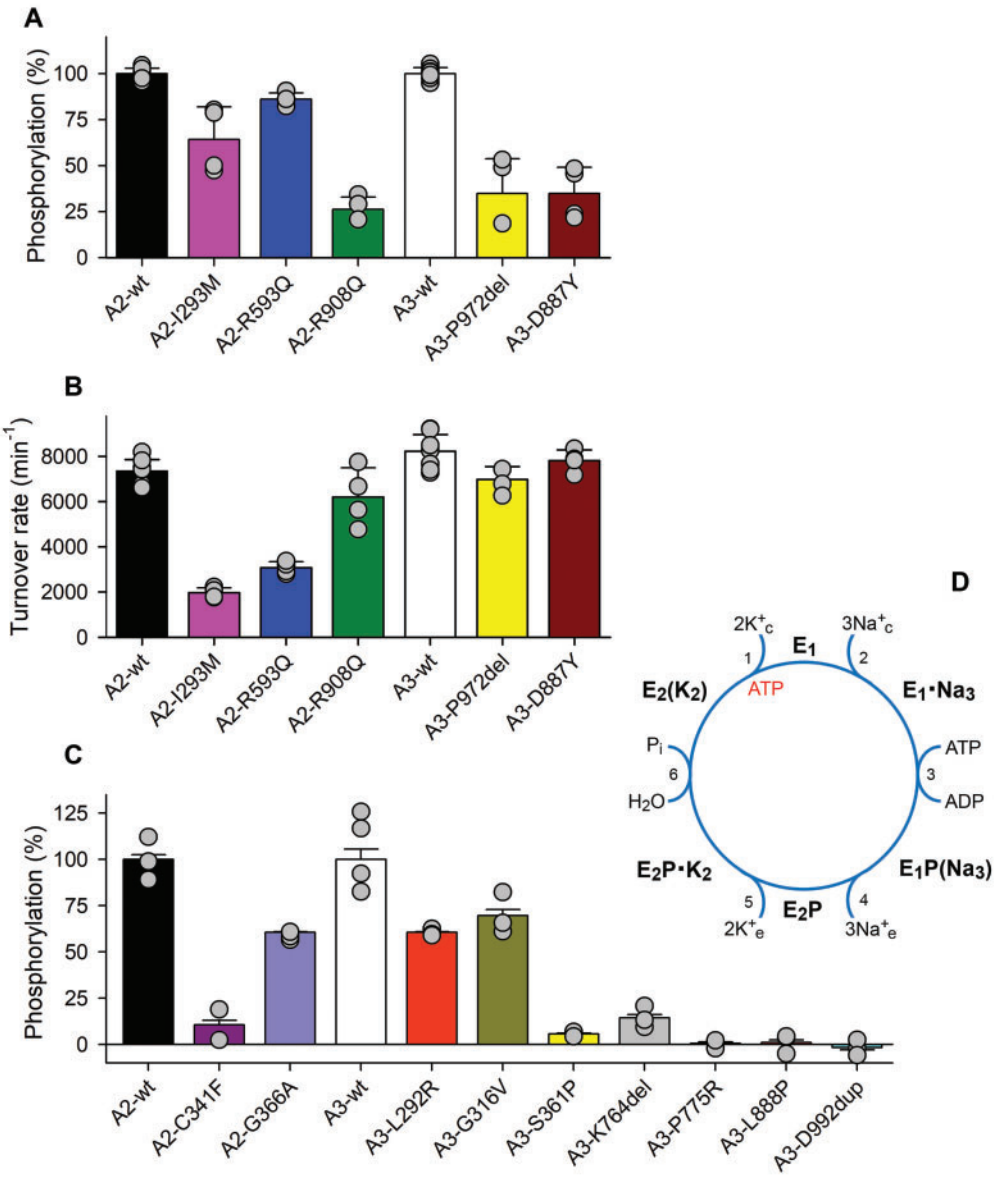

Figure 5 Relative phosphorylation/expression and turnover rate for ATPase activity with NKA reaction cycle. (**A**) Phosphorylation level of stably expressed ATP1A2 and ATP1A3 wild-type and mutants. The phosphorylation level (pmol/mg total plasma membrane protein) is shown in per cent of wild-type. Phosphorylation was determined under stoichiometric conditions, thus reflecting the expression level ('active site concentration'). (**B**) Turnover rate (min^{-1}) determined by relating the maximum NKA activity to the phosphorylation level. (**C**) Phosphorylation level of transiently expressed ATP1A2 and ATP1A3 wild-type and mutants determined as described for **A**. The NKA activity per mg total plasma membrane protein, calculated by multiplying the turnover rate by the phosphorylation level, was 17% (A2-I293M), 36% (A2-R593Q), 22% (A2-R908Q), 30% (A3-P972del), and 33% (A3-D887Y), relative to wild-type, indicating that the function of these mutants was substantially impaired despite their ability to support cell growth. (**D**) Reaction cycle of NKA. E1 and E1P are Na^+ selective conformations, whereas E2 and E2P are K^+ selective conformations. Phosphorylation by ATP (indicated by 'P'). The cytoplasmic and extracellular sides are indicated by c and e, respectively. For a detailed description see Supplementary Fig. 5 legend.[3]

motor skills. Prolonged seizure-related apnoeic episodes were a recurrent feature in five additional individuals, all exhibiting *ATP1A3* mutations. In two further patients with *ATP1A3* mutations, similar apnoeic episodes lacked any electrographic correlate and were classified as central apnoeas. In these patients, structure of the brainstem was intact, suggesting a disturbance of respiratory system regulation.

Respiratory disturbances have been described in *ATP1A3*-AHC.[30] Biallelic *ATP1A2* mutations have also been associated with respiratory failure due to absence of spontaneous respiratory effort[12,13] resembling knockout *Atp1a2* or *Atp1a3* mice, whose defective respiratory rhythm generation was attributed to failed Cl^- clearance through the K-Cl transporter (KCC2) in brainstem postsynaptic neurons.[33,34]

Downloaded from https://academic.oup.com/brain/advance-article/doi/10.1093/brain/awab052/6242725 by Universita degli Studi di Ferrara - Biblioteca S. Maria delle Grazie user on 27 April 2021

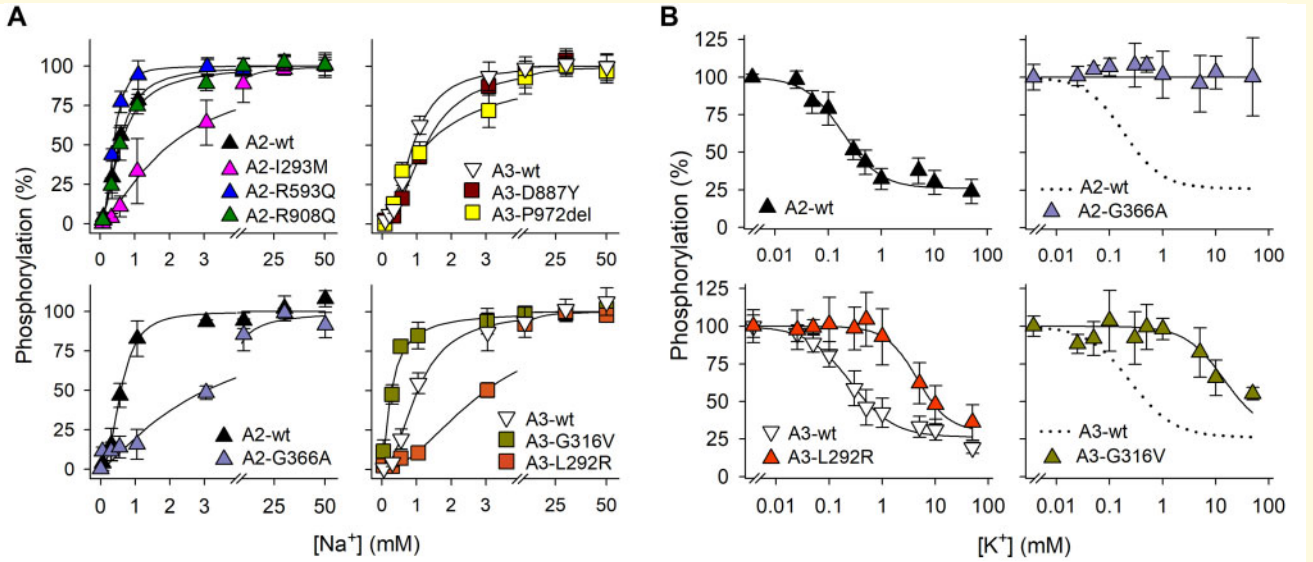

Figure 6 Na^+ and K^+ affinity of ATP1A2/A3 mutants. (**A**) Na^+ affinity determined from Na^+ activation of phosphorylation. The binding of three Na^+ to the E1 form activates phosphorylation from ATP. Phosphorylation was measured at the indicated concentrations of Na^+. Symbols with error bars represent mean ± standard deviation (SD). Each line represents the best fit of a Hill equation. The apparent Na^+ affinities ($K_{0.5}$ values) and Hill coefficients (n_H) were as follows. Stable expression (*top row*): A2-wt (wild-type), 534 ± 52 μM (n_H = 2.0); A2-I293M, 2790 ± 592 μM (n_H = 1.7); A2-R593Q, 384 ± 24 μM (n_H = 2.6); A2-R908Q, 601 ± 81 μM (n_H = 1.7); A3-wt, 916 ± 105 μM (n_H = 2.4); A3-D887Y, 1260 ± 93 μM (n_H = 2.1); A3-P972del, 1331 ± 303 μM (n_H = 1.2). Transient expression (*bottom row*): A2-wt, 595 ± 80 μM (n_H = 2.5); A2-G366A, 3079 ± 192 μM (n_H = 1.3); A3-wt, 1120 ± 127 μM (n_H = 2.1); A3-L292R, 3013 ± 254 μM (n_H = 1.9); A3-G316V, 272 ± 47 μM (n_H = 1.3). The apparent Na^+ affinity was reduced 3–5-fold ($K_{0.5}$ increased) for A2-I293M, A2-G366A, and A3-L292R, and increased 4-fold for A3-G316V ($K_{0.5}$ decreased). For A3-P972del, the cooperativity of Na^+ binding at the three sites was severely reduced (Hill coefficient 1.2 versus 2.4 for the wild-type). (**B**) K^+ affinity determined from K^+ inhibition of phosphorylation. Accumulation of phosphoenzyme is inhibited by K^+, because K^+ activates dephosphorylation of E2P and competes with Na^+ for binding to E1 (*cf.* reaction cycle in Fig. 5). Phosphorylation was measured at the indicated concentrations of K^+ on transiently expressed NKA enzyme. Symbols with error bars represent mean ± SD. Each line represents the best fit of the Hill equation for inhibitory ligand binding.[27] The apparent K^+ affinities ($K_{0.5}$ values) were as follows: A2-wt, 188 ± 43 μM; A2-G366A, > 100 mM; A3-wt, 281 ± 63 μM; A3-L292R, 4570 ± 700 μM; A3-G316V, > 10 mM. Hence, A3-L292R and A3-G316V showed 16- and > 35-fold reduction of apparent K^+ affinity, and A2-G366A was totally insensitive to K^+.

The KCC2 transporter relies on the K^+ gradient created by the NKA to pump Cl^- out of the cells. The same pathophysiological mechanism might cause the nonepileptic episodic respiratory disturbances in Patients 14 and 18.

Patients with *ATP1A3*-related disease are at increased risk of exhibiting dynamic ECG abnormalities, a finding substantiated by the multiple cardiac rhythm abnormalities observed the in murine *Atp1a3* model.[35] However, while sudden seizure-related cardiac death has been induced in murine *Atp1a3*-related disease, premature mortality remained limited to 2% in the international AHC-*ATP1A3* registry cohort over a 20 years period,[36] mainly as a consequence of accidental events or respiratory complications of status epilepticus. In our series, a short QT interval, an ECG abnormality that is potentially predisposing to life threatening arrhythmia, was present in one patient (Patient 13) and was the only abnormal finding observed among 19 patients whose ECGs were available for inspection. This patient's mutation, the A3-D801N, a highly recurrent AH mutation, was also present in one patient with AH and short QT reported by Balestrini et al.[35] The six patients with *ATP1A3* mutations who died prematurely in our series had normal ECGs. These patients died either as a consequence of an intercurrent respiratory infection or during status epilepticus after progressive worsening of their conditions. These circumstances of death were not consistent with a sudden cardiac event but it cannot be excluded that a compromised cardiac function might have contributed to these patients' vulnerability.

Brain MRI abnormalities and neuropathological findings

Polymicrogyria, which we observed with consistent features in 10 patients (45%), is a novel phenotype for heterozygous *ATP1A2* and *ATP1A3* mutations. It is possible that previously reported patients may not have had adequate MRI imaging and thus subtle alterations of the cortical folding might have been overlooked in older studies. In addition, phenotype-guided genetic testing, largely applied in the past, might have prevented novel malformation phenotypes from being found.

In one qualitative MRI study, brain and cerebellar atrophy were reported in up to 50% of patients with *ATP1A3*-

Downloaded from https://academic.oup.com/brain/advance-article/doi/10.1093/brain/awab052/6242725 by Universita degli Studi di Ferrara - Biblioteca S. Maria delle Grazie user on 27 April 2021

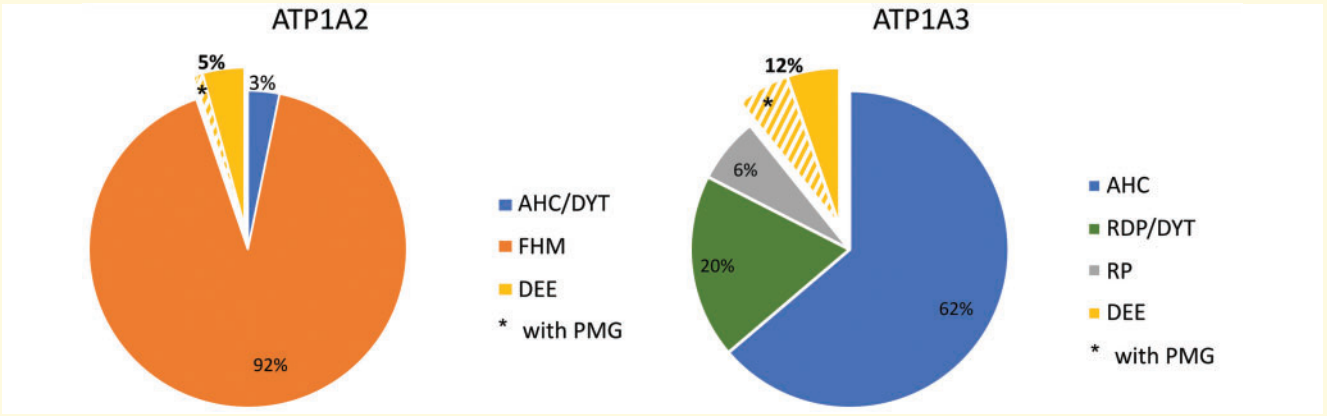

Figure 7 Distribution of ATP1A2/A3 mutations across their associated phenotypes. The pie charts show the distribution of heterozygous mutations of *ATP1A2* (*left*) and *ATP1A3* (*right*) across their associated phenotypes. We identified 92 *ATP1A2* and 136 *ATP1A3* heterozygous mutations in the Human Gene Mutation Database (https://portal.biobase-international.com), and stratified them based on the reported phenotypes, adding to previously published data the 11 novel mutations (two in *ATP1A2* and nine in *ATP1A3*) we reported in this series. Collectively, up to 5% of *ATP1A2* (6/94) and 12% of *ATP1A3* (18/145) mutations can be associated with developmental and epileptic encephalopathy. Polymicrogyria can be associated with 1% of *ATP1A2* and 5.5% of *ATP1A3* mutations (yellow-dashed area). DYT = dystonia; DEE = developmental and epileptic encephalopathy (this term includes epileptic encephalopathies and developmental encephalopathies with epilepsy); PMG = polymicrogyria; RDP = rapid-onset dystonia-parkinsonism; RP = rare phenotypes [this subgroup includes CAPOS (cerebellar ataxia-areflexia-progressive optic atrophy), RECA (relapsing encephalopathy with cerebellar ataxia), ataxia and non-specified nervous system abnormalities].

AHC.[37] Microcephaly with rapidly progressive brain atrophy was described in a single patient with *ATP1A3*-related DEE.[11] Two quantitative MRI studies in small series confirmed reduced total brain volume, with prevalent white matter involvement[38] and mild, possibly age related, cerebellar atrophy.[39]

Polymicrogyria is aetiologically heterogeneous and variable in topography.[40] In this series, the malformation was either limited to the perisylvian cortex or more diffuse but perisylvian predominant. Its characteristics shared similarities with those observed with mutations in several developmental genes (the microcephaly gene *WDR62*, multiple tubulin genes, the PIK3CA-AKT pathway associated *PIK3R2* gene), but recently also associated with the ion channel genes *SCN3A*[41,42] and, in more severe forms, *GRIN1* and *GRIN2B*.[43,44]

Mutations of *SCN3A* were initially associated with non-malformation epilepsy and DEE (MIM #617935; MIM #617938), and more recently with polymicrogyria.[41,42] However, mutations associated with polymicrogyria proved to be gain-of-function resulting in increased non-inactivating persistent Na^+ currents ($I\text{-}Na_P$). Changes in the sodium flux in glia and neurons may reverse Na^+/Ca^{2+} exchangers triggering calcium waves.[41,42]

In *GRIN1*-associated polymicrogyria, gain-of-function mutations causing hyperactivation of NMDA receptors increase intracellular Ca^{2+}, which was predicted to induce polymicrogyria either by causing increased cell death during foetal brain development (excitotoxicity) or by activating signalling pathways such as PI3K-AKT.[43] A similar mechanism would be at play with *GRIN2B* mutations.[45] Altered NMDA receptor-mediated calcium mobilization disturbs neuronal migration in a mouse model of Zellweger syndrome, a rare metabolic disorder featuring a polymicrogyria-like cortical malformation.[46] The altered functioning of the NKA pump provides further evidence that changes in ion homeostasis during embryogenesis may disrupt cortical development.[45]

One child from a large family segregating FHM (A2-R348P) was reported to have lissencephaly with microcephaly and retinal dysplasia, likely an unrelated phenotype.[47] One of the mutations found in our series has been reported in ~40% of individuals with AHC (Patient 13: A3-D801N) with no brain malformation reported.[18] Different phenotypes associated to the same mutation are not new to *ATP1A3*. The D923N mutation is recurrent in RDP but has also been observed in one family with four affected individuals with alternating hemiplegia.[48] These authors postulated that these clinical syndromes represent the different expressions of the same disorder and that the specific *ATP1A3* mutation is not the only determinant of clinical expression, implying that genetic, epigenetic, and environmental factors may all influence clinical expression of *ATP1A3* related disease. The A2-R908Q mutation was associated with early onset epileptic encephalopathy in one patient in our series and with familial hemiplegic migraine in multiple unrelated individuals in the literature,[19,49,50] demonstrating that phenotypic heterogeneity is not limited to *ATP1A3* mutations.

We observed variable expressivity for polymicrogyria with one mutation in our series, in which two unrelated individuals carrying the same *ATP1A3* mutation (Patients 9 and 20: A3-S361P) had early onset DEE and microcephaly, associated with polymicrogyria and alternating hemiplegia only in

Downloaded from https://academic.oup.com/brain/advance-article/doi/10.1093/brain/awab052/6242725 by Universita degli Studi di Ferrara - Biblioteca S. Maria delle Grazie user on 27 April 2021

one (Patient 20). We also observed incomplete penetrance and variable expressivity within a single family in which the proband (Patient 14: A3-D887Y) had early onset DEE and bilateral polymicrogyria, his mother (Patient 15) had migraine, mild intellectual disability and unilateral polymicrogyria, and the maternal grandfather had no reported symptoms and a normal brain MRI despite carrying a germline mutation. Incomplete penetrance and variable expressivity have also been observed with *SCN3A*-associated polymicrogyria.[41] Similarly, *GRIN1* mutations even within the same functional domain can result in DEE with normal MRI or polymicrogyria.[43]

Neuropathological study of the whole brain in Patients 11 (A3-K764del) and 23 (homozygous A2-R279Gfs*4), displayed substantially similar findings. The most obvious similarities were small size of the hemispheres with widespread polymicrogyria covered by extensive leptomeningeal glioneuronal heterotopia, confirmed histologically in both brains. Also, the white matter was atrophic and the corpus callosum small, suggesting that cortical axons were deficient. The most striking difference between the two brains were the abundant mineralizations seen in the brain and blood vessels of Patient 23, which were not observed in Patient 11. Extensive vascular and parenchymal mineralization was also reported in previous clinical and pathological studies of patients with polymicrogyria and biallelic *ATP1A2* mutations.[12] These findings suggest that *ATP1A2* may be important for development and function of both neural and vascular tissue in the brain.

The known expression patterns of *ATP1A2* and *ATP1A3* support the microcephaly and polymicrogyria seen in our series (mouse: http://www.informatics.jax.org; human: http://www.hdbr.org/expression). In developing mouse brain, *Atp1a2* is highly expressed in neural progenitors and meninges, then persists after birth in glial cells.[5,6,51] *Atp1a3* is also expressed in neural progenitors but not in meninges and persists after birth in postnatal neurons.[5,51] Thus, both genes could be implicated in direct injury to radial glia and migrating neurons. In sum, the expression patterns of *ATP1A2/A3* in developing brain combined with observations in two brains from our series support a mainly neural (radial glia, progenitors, migrating neurons) pathogenesis that may be compounded by meningeal and vascular abnormalities. No obvious brain anatomical defects have been reported in *ATP1A2/A3* mouse models.[33,34] However, mouse models are not particularly suitable to unveil abnormal cortical folding and defective cortical lamination might have remained unnoticed as no specific studies seem to have investigated it.

Different studies have suggested a direct link between the Na+,K+-ATPase and signal transduction pathways involving, among others, the Src family kinases, and PI3K, which has been implicated in a spectrum of brain malformations. According to these studies, the transmembrane NKA pump would act as a scaffold, tethering signalling proteins together into distinct cellular compartments, thus contributing to the modulation of signal transduction within the cell.[52]

Structural and functional considerations

A clustering of AHC-associated *ATP1A3* mutations in transmembrane domains 2–9 has been previously reported.[3,30] Conversely, FHM-associated *ATP1A2* mutations and RDP-associated *ATP1A3* mutations are scattered throughout the protein.[3,30]

In our cohort we observed an enrichment of *ATP1A3* mutations in transmembrane domains M3-M10 clustered around the ion binding sites (8/14; Supplementary Fig. 3), as previously noted for AHC-associated mutations, suggesting that the most severe *ATP1A3*-related phenotypes may be associated with this location.[53] There was no clustering distribution of *ATP1A2* mutations in our series, although the A2-G366A mutation, affecting the P domain, was recurrent in two unrelated patients with super-refractory status epilepticus who died prematurely (Patients 3 and 4).

Most of the mutations found in our cohort result in severe functional defects based on both disruption of protein structure and biochemical analysis. Many of the mutations replace or insert bulky and/or charged residues such as aromatic amino acids, proline or arginine with smaller or less charged residues, while a few simply delete or duplicate a residue. All 14 of the mutations we tested caused reduced NKA pump activity in the COS-1 cellular model. In nine mutants the NKA pump activity was too low for survival of the transfected COS-1 cells, substantiating the 'profound' phenotypes featuring early death, DEE, progressive brain atrophy and polymicrogyria observed in most patients carrying these mutations (Table 1). The very low pump activity results from severely reduced expression level, inability to form a phosphoenzyme or, for the phosphorylatable mutants A3-L292R, A3-G316V and A2-G366A, a severe reduction in Na^+ and/or K^+ affinity. The remaining five mutations caused reduced (17–36%) activity that was sufficient for cell growth, attributed to either reduced expression level in the plasma membrane (A2-R908Q, A3-P972del, and A3-D887Y), or an E1P shift of the E1P-E2P conformational equilibrium (A2-I293M, A2-R593Q).

Based on the impaired NKA pump activity observed in the COS-1 cells, where only the mutant NKA is expressed, we classify the mutations in our cohort as loss-of-function, including those mutants for which the impaired pump activity is due to reduced plasma membrane targeting, as previously indicated for A2-R908Q.[54]

Dominant negative effects, which have previously been suggested for A3-D801N (Patient 3), A3-E815K and A3-G947R[24] may also be contributing to the severe phenotype in our series. A number of factors argue against haploinsufficiency as the main pathogenetic mechanism, including absence of phenotypic manifestations in carrier parents, similarities of the neuropathological polymicrogyria phenotype with that observed with biallelic mutations (Patient 23)[12] and the non-malformative phenotypes observed in individuals with large deletions involving *ATP1A2/A3* (DECIPHER, https://decipher.sanger.ac.uk/; ClinVar, https://

Downloaded from https://academic.oup.com/brain/advance-article/doi/10.1093/brain/awab052/6242725 by Universita degli Studi di Ferrara - Biblioteca S. Maria delle Grazie user on 27 April 2021

www.ncbi.nlm.nih.gov/clinvar/). Misfolding of the mutant α-subunit and allele competition for the β-subunit might also contribute to deleteriousness of *ATP1A3* mutations and their phenotypic heterogeneity.[26]

Sweadner et al.[53] suggested that genes that only diverged slightly after past duplications, such as *ATP1A2* and *ATP1A3*, would be expected to harbour similar pathogenic mutations, but observed that only relatively few mutations affected the corresponding amino acids in these two genes. Our study provides additional examples of mutations affecting homologous residues in *ATP1A2* and *ATP1A3* (Supplementary Table 2). The ATP1A2 glycine 366 (A2-G366), which is mutated in Patients 3 and 4 (A2-G366A) with early lethal phenotypes, corresponds to the G358 residue in ATP1A3 mutated in a newborn with seizures and progressive brain atrophy who died prematurely (G358V).[11] Different *de novo* substitutions of A2-G366 have been reported in one patient with refractory epilepsy (A2-G366V)[10] and in another with a non-specific neurodevelopmental disorder (A2-G366C).[55] A2-G366, or its equivalent in ATP1A3, is located in the P-domain at the junction between the P1-helix and the P1-β-strand leading directly to the phosphorylated active site aspartate of the DKTGT motif (Supplementary Fig. 6). The glycine is important for the direction of this β strand. In COS-1 cells transfected with the A3-G366A, the NKA showed a 5-fold reduction in Na^+ affinity and a highly reduced apparent K^+ affinity too, with lack of transport activity due to lack of K^+-induced dephosphorylation of E2P.

Genotype-phenotype analysis

The phenotypes observed in our cohort were predominately severe, with short survival (death at 0–3 years) observed in 7/22 (32%), severe congenital or postnatal microcephaly in 10/22 (45%), polymicrogyria in 10/22 (45%), and severe or profound early developmental delay or intellectual disability in 14/18 (78%) individuals. We tested 14 mutations from 17 patients and next separated our patient cohort into two groups based on COS-1 cell survival in ouabain selection pressure (Table 1). Group 1 included 11 patients harbouring nine different mutations, all resulting in lack of cell survival; we observed early mortality in 5/11 (45%), severe microcephaly in 6/11 (55%), polymicrogyria in 5/11 (45%) and severe or profound intellectual disability in 8/9 (89%) patients. Group 2 included six patients whose mutations were associated with cell survival; we found early mortality and severe microcephaly in only 1/6 (17%) each, polymicrogyria in 3/6 (50%) and severe or profound intellectual disability in 2/6 (33%) patients. A comparison of the two groups suggests a trend toward more severe phenotype in Group 1, but the differences were not statistically significant due to small numbers (Fisher's exact test). Further, all the phenotypes in both groups were relatively severe, which fits with our finding of severe functional defects in various experimental paradigms for all mutations (Table 1).

For example, seven children (five from Group 1, one from Group 2, and a further patient with the untested A3-G893W) died at 0–3 years with profound encephalopathies classified as DEE. In Group 1, two individuals without polymicrogyria carried the severe A2-G366A mutation, while the remaining three all had polymicrogyria with mutations affecting the transmembrane helices (A3-L292R, A3-K764del, and A3-D992dup) and causing severe impairment of NKA pump activity. A3-L292R caused severe reduction of Na^+ and K^+ affinity, compatible with the location of the bulky, positively charged arginine substituent in position to repel Na^+ and K^+ at their binding sites (Supplementary Fig. 9). For A3-K764del and A3-D992dup, phosphorylation and expression were very low or undetectable, most likely caused by misfolding and/or disruption of Na^+ binding, as these residues are involved in an intricate hydrogen bonding network that is essential for positioning of the transmembrane helices and C-terminus forming the fold for Na^+ binding at site III (Supplementary Fig. 10).

The remaining 15 subjects survived infancy although one later died at 14 years. We tested 10 mutations from this group, including five (A2-C341F, A3-G316V, A3-S361P, A3-P775R, A3-L888P) that resulted in loss of NKA pump activity as indicated by lack of COS-1 cell survival. The six children harbouring these five mutations all had severe phenotypes that included intractable epilepsy and severe intellectual disability, variably associated with microcephaly, polymicrogyria and alternating hemiplegia (A3-L888P and A3-S361P), severe hypotonia, and/or progressive brain atrophy (A2-C341F, A3-G316V, A3-S361P). The two patients with alternating hemiplegia in this group (Patients 16 and 20) were the only ones to manifest this disorder in the entire series. However, recognition of attacks may have been hampered by severe hypotonia and frequent seizures in the other children. In Patient 8: A3-G316V, the low pump activity was associated with low K^+ affinity, compatible with insertion of a bulky valine close to the ion binding sites (Supplementary Fig. 9). Phosphorylation and expression were very low or undetectable for A2-C341F, A3-S361P, A3-P775R, and A3-L888P. For A3-S361P, the lack of phosphorylation most likely results from redirection of the β-strand leading to the phosphorylated aspartate by insertion of a proline five residues before the aspartate (Supplementary Fig. 6). For A2-C341F and A3-P775R, the inserted bulky side chains appear to disturb ion binding and helix packing in the membrane, especially when charged arginine is involved (Supplementary Fig. 5 and 9). A3-L888P inserts a proline redirecting the L7-8 loop, predicted to disrupt the interaction between the α- and β-subunits, which should prevent expression in the plasma membrane (Supplementary Fig. 8).

The remaining five mutations resulted in partially conserved NKA pump activity allowing long term COS-1 cell survival. In the six subjects harbouring these mutations, the phenotypes were of variable severity. Three patients (Patient 6: A2-R908Q; Patients 14 and 15: A3-D887Y; Patient 18: A3-P972del) had severe phenotypes that overlap with those associated with COS-1 lethal mutations, including severe

Downloaded from https://academic.oup.com/brain/advance-article/doi/10.1093/brain/awab052/6242725 by Universita degli Studi di Ferrara - Biblioteca S. Maria delle Grazie user on 27 April 2021

hypotonia and polymicrogyria. In COS-1 cells, these mutations led to reduced expression in the plasma membrane by interference with the α-β interaction (Supplementary Fig. 8) leading to retention of immature protein in the endoplasmic reticulum and/or decreased stability. The ATP1A3 residue homologous to A2-R908 is targeted by an AHC mutation (A3-R901T)[3] and the ATP1A2 residue homologous to A3-G893 is targeted by a hemiplegic migraine mutation (A2-G900R).[31] The remaining three patients had less severe phenotypes consisting of mild-moderate intellectual disability with mild focal epilepsy (Patient 1: A2-I293M; Patient 5: A2-R593Q) or unilateral polymicrogyria and migraine (Patient 15: A3-D887Y). The less severe phenotypes associated with A2-I293M and A2-R593Q may be related to their near normal expression level, which suggests a relatively stable protein, combined with retention of NKA pump activity, albeit with reduced maximal turnover rate.

Patient 21 carried the A3-F857del in 26.2% of WES reads. Mosaicism for *ATP1A3* mutations has been reported in a single AHC patient with VAF 44% and a mild phenotype and in six asymptomatic parents of AHC probands (VAF <18.82%).[56] The phenotype of Patient 21 was severe despite the mosaic state of the mutation, which is likely to affect the interaction between M7 and the transmembrane helix of the β-subunit.

Conclusion

This series links profound early lethal phenotypes with COS-1 lethal mutations, but also reveals a continuum of phenotypic severity, in which both severe and milder phenotypes can be associated with mutations partially sparing NKA pump function, while polymicrogyria is distributed across mutations of variable effect. The molecular diagnostic yield of polymicrogyria is low, with multiple genes accounting for a small number of diagnoses each, and a relevant number of patients resulting from non-genetic, mainly vascular or infective, prenatal causes.[40,57,58] The proportion of patients with polymicrogyria related to *ATP1A2/A3* remains unknown since available next generation studies on malformations of cortical development have been either performed with gene panels which included neither of the two genes[59] or carrying out WES in small series in which no pathogenic variants in either gene emerged.[57,60] This study widens the clinical spectrum of ATP1A2/A3-opathies to include profound epilepsy phenotypes, with and without associated polymicrogyria. Inclusion of *ATP1A2/A3*, in virtual panels used to interrogate WES/WGS data and in targeted-gene diagnostic panels for polymicrogyria and DEE will clarify the magnitude of their role in large series with these disorders.

Acknowledgements

We thank Nina Juste and Randi Scheel, Aarhus University, for expert technical assistance. We also thank Mrs Diana Bazan for her skilful technical assistance (Neuropathology). This work was generated within the European Reference Networks EpiCARE and ITHACA.

Funding

This work was supported by grants to B.V. from the Lundbeck Foundation (grant R223-2016-595) and the Danish Medical Research Council (grant 7016-00193B), grants to R.G. from the European Union Seventh Framework Programme FP7/2013 under the project DESIRE (grant 602531), the Italian Ministry of Health and Tuscany Region (grant RF-2013-02355240), the Tuscany Region Call for Health 2018 (grant DECODE EE) and grants to I.E.S. from the National Health and Medical Research Council of Australia (grants APP1091593, APP1104831).

Competing interests

The authors report no competing interests.

Appendix 1

ATP1A2/A3-collaborators. Full details are provided in the Supplementary material.

Damien Sanlaville, Rani Sachdev, Ian Andrews, Francesco Mari, Anna Cavalli, Carmen Barba, Beatrice De Maria, Giampaolo Garani, Johannes R. Lemke, Mario Mastrangelo, Emily Tam, Elizabeth Donner, Helen Branson, Fabiola P. Monteiro, Fernando Kok, Katherine B. Howell, Stephanie Leech, Heather Mefford, Alison Muir.

Supplementary material

Supplementary material is available at *Brain* online.

References

1. Kaplan JH. Biochemistry of Na,K-ATPase. *Annu Rev Biochem*. 2002;71:511-535.
2. Friedrich T, Tavraz NN, Junghans C. ATP1A2 mutations in migraine: seeing through the facets of an ion pump onto the neurobiology of disease. *Front Physiol*. 2016;7:1-21.
3. Holm R, Toustrup-Jensen MS, Einholm AP, et al. Neurological disease mutations of α3 Na+,K+-ATPase: structural and functional perspectives and rescue of compromised function. *Biochim Biophys Acta Bioenerg*. 2016;1857:1807-28.
4. Blanco G. Na, K-ATPase subunit heterogeneity as a mechanism for tissue-specific ion regulation. *Semin Nephrol*. 2005;25:292-303.
5. McGrail KM, Phillips JM, Sweadner KJ. Immunofluorescent localization of three Na,K-ATPase isozymes in the rat central nervous system: both neurons and glia can express more than one Na,K-ATPase. *J Neurosci*. 1991;11:381-391.

Downloaded from https://academic.oup.com/brain/advance-article/doi/10.1093/brain/awab052/6242725 by Universita degli Studi di Ferrara - Biblioteca S. Maria delle Grazie user on 27 April 2021

6. Moseley AE, Lieske SP, Wetzel RK, et al. The Na,K-ATPase α2 isoform is expressed in neurons, and its absence disrupts neuronal activity in newborn mice. *J Biol Chem*. 2003;278:5317-5324.
7. Bassi MT, Bresolin N, Tonelli A, et al. A novel mutation in the ATP1A2 genes causes alternating hemiplegia of childhood. *J Med Genet*. 2004.
8. Swoboda KJ, Kanavakis E, Xaidara A, et al. Alternating hemiplegia of childhood or familial hemiplegic migraine?: a novel ATP1A2 mutation. *Ann Neurol*. 2004;55:884-887.
9. Dard R, Mignot C, Durr A, et al. Relapsing encephalopathy with cerebellar ataxia related to an ATP1A3 mutation. *Dev Med Child Neurol*. 2015;57:1183-1186.
10. Liu J, Tong L, Song S, et al. Novel and de novo mutations in pediatric refractory epilepsy. *Mol Brain*. 2018;11:18.
11. Paciorkowski AR, McDaniel SS, Jansen LA, et al. Novel mutations in ATP1A3 associated with catastrophic early life epilepsy, episodic prolonged apnea, and postnatal microcephaly. *Epilepsia*. 2015; 56:422-430.
12. Chatron N, Cabet S, Alix E, et al. A novel lethal recognizable polymicrogyric syndrome caused by ATP1A2 homozygous truncating variants. *Brain*. 2019;142:3367-3374.
13. Monteiro FP, Curry CJ, Hevner R, et al. Biallelic loss of function variants in ATP1A2 cause hydrops fetalis, microcephaly, arthrogryposis and extensive cortical malformations. *Eur J Med Genet*. 2020;63:103624.
14. Scheffer IE, Berkovic S, Capovilla G, et al. ILAE classification of the epilepsies: position paper of the ILAE commission for classification and terminology. *Epilepsia*. 2017;58:512-521.
15. Burgess R, Wang S, McTague A, et al.; EIMFS Consortium. The genetic landscape of epilepsy of infancy with migrating focal seizures. *Ann Neurol*. 2019;86:821-831.
16. Heinzen EL, Swoboda KJ, Hitomi Y, et al. European Alternating Hemiplegia of Childhood (AHC) Genetics Consortium. De novo mutations in ATP1A3 cause alternating hemiplegia of childhood. *Nat Genet*. 2012;44:1030-1034.
17. Marzin P, Mignot C, Dorison N, et al. Early-onset encephalopathy with paroxysmal movement disorders and epileptic seizures without hemiplegic attacks: about three children with novel ATP1A3 mutations. *Brain Dev*. 2018;40:768-774.
18. Rosewich H, Thiele H, Ohlenbusch A, et al. Heterozygous de-novo mutations in ATP1A3 in patients with alternating hemiplegia of childhood: a whole-exome sequencing gene-identification study. *Lancet Neurol*. 2012;11:764-773.
19. De Vries B, Freilinger T, Vanmolkot KRJ, et al. Systematic analysis of three FHM genes in 39 sporadic patients with hemiplegic migraine. *Neurology*. 2007;69:2170-2176.
20. Retterer K, Juusola J, Cho MT, et al. Clinical application of whole-exome sequencing across clinical indications. *Genet Med*. 2016;18:696-704.
21. Panagiotakaki E, de Grandis E, Stagnaro M, et al. The Italian IBAHC Consortium. Clinical profile of patients with ATP1A3 mutations in alternating hemiplegia of childhood—a study of 155 patients. *Orphanet J Rare Dis*. 2015;10:123. doi: 10.1186/s13023-015-0335-5.
22. Parrini E, Marini C, Mei D, et al. Clinical Study Group. Diagnostic targeted resequencing in 349 patients with drug-resistant pediatric epilepsies identifies causative mutations in 30 different genes. *Hum Mutat*. 2017;38:216-225.
23. Ueda K, Serajee F, Huq AM. Clinical benefit of NMDA receptor antagonists in a patient with ATP1A2 gene mutation. *Pediatrics*. 2018;141:S390-S394.
24. Li M, Jazayeri D, Corry B, et al. A functional correlate of severity in alternating hemiplegia of childhood. *Neurobiol Dis*. 2015;77: 88-93.
25. Weigand KM, Messchaert M, Swarts HGP, et al. Alternating hemiplegia of childhood mutations have a differential effect on Na+,K+-ATPase activity and ouabain binding. *Biochim Biophys Acta Mol Basis Dis*. 2014;1842:1010-1016.
26. Arystarkhova E, Haq IU, Luebbert T, et al. Factors in the disease severity of ATP1A3 mutations: impairment, misfolding, and allele competition. *Neurobiol Dis*. 2019;132:104577.
27. Nielsen HN, Spontarelli K, Holm R, et al. Distinct effects of Q925 mutation on intracellular and extracellular Na+ and K+ binding to the Na+, K+-ATPase. *Sci Rep*. 2019;9:13344.
28. De Carvalho Aguiar P, Sweadner KJ, Penniston JT, et al. Mutations in the Na+/K+-ATPase α3 gene ATP1A3 are associated with rapid-onset dystonia parkinsonism. *Neuron*. 2004;43: 169-175.
29. De Fusco M, Marconi R, Silvestri L, et al. Haploinsufficiency of ATP1A2 encoding the Na+/K+ pump α2 subunit associated with familial hemiplegic migraine type 2. *Nat Genet*. 2003;33:192-196.
30. Rosewich H, Ohlenbusch A, Huppke P, et al. The expanding clinical and genetic spectrum of ATP1A3-related disorders. *Neurology*. 2014;82:945-955.
31. Deprez L, Weckhuysen S, Peeters K, et al. Epilepsy as part of the phenotype associated with ATP1A2 mutations. *Epilepsia*. 2008; 49:500-508.
32. Prontera P, Sarchielli P, Caproni S, et al. Epilepsy in hemiplegic migraine: genetic mutations and clinical implications. *Cephalalgia*. 2018;38:361-373.
33. Ikeda K, Onaka T, Yamakado M, et al. Degeneration of the amygdala/piriform cortex and enhanced fear/anxiety behaviors in sodium pump α2 subunit (Atpla2)-deficient mice. *J Neurosci*. 2003; 23:4667-4676.
34. Ikeda K, Onimaru H, Kawakami K. Knockout of sodium pump α3 subunit gene (Atp1a3–/–) results in perinatal seizure and defective respiratory rhythm generation. *Brain Res*. 2017;1666:27-37.
35. Balestrini S, Mikati MA, Garcia-Roves RA, et al. Cardiac phenotype in ATP1A3-related syndromes: a multicentre cohort study. *Neurology*. 2020;95:e2866-e2879.
36. Rosewich H, Sweney MT, Debrosse S, et al. Research conference summary from the 2014 International Task Force on ATP1A3-related disorders. *Neurol Genet*. 2017;3:e139.
37. Sasaki M, Ishii A, Saito Y, et al. Progressive brain atrophy in alternating hemiplegia of childhood. *Mov Disord Clin Pract*. 2017;4: 406-411.
38. Severino M, Pisciotta L, Tortora D, et al. The IBAHC Consortium. White matter and cerebellar involvement in alternating hemiplegia of childhood. *J Neurol*. 2020;267:1300-1311.
39. Ghusayni R, Richardson JP, Uchitel J, et al. Magnetic resonance imaging volumetric analysis in patients with Alternating hemiplegia of childhood: a pilot study. *Eur J Paediatr Neurol*. 2020;26:15-19.
40. Guerrini R, Dobyns WB. Malformations of cortical development: clinical features and genetic causes. *Lancet Neurol*. 2014;13: 710-726.
41. Smith RS, Kenny CJ, Ganesh V, et al. Sodium channel SCN3A (NaV1.3) regulation of human cerebral cortical folding and oral motor development. *Neuron*. 2018;99:905-13.e7.
42. Zaman T, Helbig KL, Clatot J, et al. SCN3A-related neurodevelopmental disorder: a spectrum of epilepsy and brain malformation. *Ann Neurol*. 2020;88:348-362.
43. Fry AE, Fawcett KA, Zelnik N, et al. De novo mutations in GRIN1 cause extensive bilateral polymicrogyria. *Brain*. 2018;141: 698-712.
44. Platzer K, Yuan H, Schütz H, et al. GRIN2B encephalopathy: novel findings on phenotype, variant clustering, functional consequences and treatment aspects. *J Med Genet*. 2017;54:460-470.
45. Smith RS, Walsh CA. Ion channel functions in early brain development. *Trends Neurosci*. 2020;43:103-114.
46. Gressens P, Baes M, Leroux P, et al. Neuronal migration disorder in Zellweger mice is secondary to glutamate receptor dysfunction. *Ann Neurol*. 2000;48:336-343.
47. Pelzer N, Blom DE, Stam AH, et al. Recurrent coma and fever in familial hemiplegic migraine type 2. A prospective 15-year follow-up of a large family with a novel ATP1A2 mutation. *Cephalalgia*. 2017;37:737-755.

Downloaded from https://academic.oup.com/brain/advance-article/doi/10.1093/brain/awab052/6242725 by Universita degli Studi di Ferrara - Biblioteca S. Maria delle Grazie user on 27 April 2021

48. Roubergue A, Roze E, Vuillaumier-Barrot S, et al. The multiple faces of the ATP1A3-related dystonic movement disorder. *Mov Disord*. 2013;28:1457-1459.
49. Blicher JU, Tietze A, Donahue MJ, et al. Perfusion and pH MRI in familial hemiplegic migraine with prolonged aura. *Cephalalgia*. 2016;36:279-283.
50. Roth C, Freilinger T, Kirovski G, et al. Clinical spectrum in three families with familial hemiplegic migraine type 2 including a novel mutation in the ATP1A2 gene. *Cephalalgia*. 2014;34:183-190.
51. Herrera VLM, Cova T, Sassoon D, et al. Developmental cell-specific regulation of Na + -K + -ATPase α1-, α2-, and α3-isoform gene expression. *Am J Physiol Cell Physiol*. 1994;266:35.
52. Reinhard L, Tidow H, Clausen MJ, et al. Na + ,K + -ATPase as a docking station: protein-protein complexes of the Na + ,K + -ATPase. *Cell Mol Life Sci*. 2013;70:205-222.
53. Sweadner KJ, Arystarkhova E, Penniston JT, et al. Genotype-structure-phenotype relationships diverge in paralogs ATP1A1, ATP1A2, and ATP1A3. *Neurol Genet*. 2019;5:e303.
54. Tavraz NN, Dürr KL, Koenderink JB, et al. Impaired plasma membrane targeting or protein stability by certain ATP1A2 mutations identified in sporadic or familial hemiplegic migraine. *Channels*. 2009;3:82-87.
55. McRae JF, Clayton S, Fitzgerald TW, et al. Prevalence and architecture of de novo mutations in developmental disorders. *Nature*. 2017;542:433-438.
56. Yang X, Yang X, Chen J, et al. ATP1A3 mosaicism in families with alternating hemiplegia of childhood. *Clin Genet*. 2019;96:43-52.
57. Mirzaa GM, Conti V, Timms AE, et al. Characterisation of mutations of the phosphoinositide-3-kinase regulatory subunit, PIK3R2, in perisylvian polymicrogyria: a next-generation sequencing study. *Lancet Neurol*. 2015;14:1182-1195.
58. Park K, Chapman T, Aldinger K, et al. The spectrum of brain malformations and disruptions in twins. *Am J Med Genet Part A*. 2020; 1–29. doi:10.1002/ajmg.a.61972.
59. Oegema R, Barakat TS, Wilke M, et al. International consensus recommendations on the diagnostic work-up for malformations of cortical development. *Nat Rev Neurol*. 2020;16:618-635.
60. Wiszniewski W, Gawlinski P, Gambin T, et al. Comprehensive genomic analysis of patients with disorders of cerebral cortical development. *Eur J Hum Genet*. 2018;26:1121-1131.

Downloaded from https://academic.oup.com/brain/advance-article/doi/10.1093/brain/awab052/6242725 by Universita degli Studi di Ferrara - Biblioteca S. Maria delle Grazie user on 27 April 2021